The g-Good-Neighbor r-Component Diagnosability of Hypercube—Theoretical and Algorithmic Approaches

Yuankang Mao, Jiafei Liu, Sun-Yuan Hsieh, *Fellow, IEEE*, Jingli Wu, and Gaoshi Li

***Abstract*—The proliferation of interconnection networks has intensified the demand for robust fault diagnosis methodologies. Although existing research focuses predominantly on single-condition diagnosability metrics, these approaches often fail to capture hybrid failure scenarios in large-scale networks. To provide a more comprehensive and realistic resilience assessment, this article introduces a new diagnosability metric termed the g-good-neighbor r-component diagnosability, denoted by $D_{g,r}(G)$. This metric imposes two stringent constraints on the network after removing a faulty node set F: i) the residual network must contain at least r connected components, and ii) every fault-free node must retain at least g fault-free neighbors. We focus on the hypercube (Q_n), a prevalent interconnection architecture renowned for its high symmetry, scalability, and fault tolerance. Under the PMC and MM$*$ diagnostic models, we establish the exact value $D_{2,2}(Q_n) = 8n - 21$ for $n \geq 24$. Leveraging the distinct characteristics of the PMC and MM$*$ models, we propose two scalable fault localization algorithms tailored for hypercube architectures. Simulation experiments on Q_n networks demonstrate that the proposed framework achieves approximately 100% true positive rate (TPR) when faulty nodes constitute $\leq 20\%$ of the network, maintaining TPR $> 98.7\%$ even as fault densities approach 50%.**

***Index Terms*—Fault diagnosis, g-good-neighbor r-component diagnosability, hypercube network, MM$*$ model, PMC model.**

I. Introduction

THE evolution of high-performance computing (HPC) systems has broadened their deployment across diverse domains, necessitating resilient interconnection architectures. The hypercube, distinguished by its structural symmetry, topological scalability, and inherent fault tolerance, constitutes a cornerstone for such infrastructures. Notably, real-world implementations underscore its practical viability: the Intel iPSC/2, a pioneering parallel computer, employs a hypercube as its underlying topology, while the HPC system SGI Origin utilizes a hypercube-based architecture as its foundational interconnection framework. As system dimensionality increases exponentially, the probability of node failures escalates accordingly, jeopardizing operational continuity. System-level diagnosis, a paradigm where nodes execute mutual tests and collectively analyze results, provides the foundational mechanism for fault tolerance. Within this framework, diagnosability, quantified as the maximum cardinality of identifiable faulty nodes, emerges as the critical determinant of system resilience. This enhanced diagnosability sustains system functionality under multiple node failure conditions by enabling precise fault localization and rapid recovery.

To derive theoretical bounds for diagnosability, diagnostic models are essential for fault diagnosis. The Preparata–Metze–Chien (PMC) model proposed in [1] and the modified Maeng–Malek (MM$*$) model established in [3] are two widely adopted frameworks. Under the PMC model, a framework based on testing principles, adjacent nodes test each other mutually and obtain outcomes. Maeng and Malek's MM model [2] functions as a test-comparison mechanism where a node sends identical tasks to two neighbors and evaluates their responses for consistency. Building on the MM model, Sengupta and Dahbura [3] provided the modified MM$*$ model, requiring nodes to test any pair of their neighbors and compare the responses. The PMC and MM$*$ models have undergone comprehensive validation within diagnosability studies, supported by numerous research findings [17], [18], [19], [20], [21], [22]. Peng et al. [4] initially explored the g-good-neighbor conditional diagnosability and proved that for a hypercube under the PMC model, it equals $(n-g+1)2^g - 1$ when $n \geq 3$ and $0 \leq g \leq n-3$. Zhang and Yang [5] proposed the concept of h-extra conditional diagnosability. Under the PMC model, with conditions $n \geq 4$ and $0 \leq h \leq n-4$, it was analyzed as $(h+1)n - h - \frac{h(h-1)}{2}$ for the hypercube. Later, the r-component conditional diagnosability was presented in [6]. Under the PMC and MM$*$ models, Zhang et al. [6] characterized that it is $-\frac{1}{2}r^2 + (n-\frac{1}{2})r + 1$ when $n \geq 7, 0 \leq r \leq n$ for the hypercube. Zhang et al. [23] suggested

Received 16 August 2025; revised 22 October 2025; accepted 21 November 2025. Date of publication 10 December 2025; date of current version 24 December 2025. This work was supported in part by the National Natural Science Foundation of China under Grant 62302107, Grant 62366007, in part by Guangxi Natural Science Foundation under Grant 2025GXNSFBA069563, 2025GXNSFAA069507, in part by Research Fund of Guangxi Key Lab of Multi source Information Mining Security under Grant 24-A-03-01 and Grant 24-A-03-02, and in part by Guangxi Young Elite Scientist Sponsorship Program under Grant GXYESS2025010. Associate Editor: S. Yin. *(Corresponding author: Jiafei Liu.)*

Yuankang Mao, Jiafei Liu, Jingli Wu, and Gaoshi Li are with the Key Lab of Education Blockchain and Intelligent Technology, Ministry of Education, Guangxi Normal University, Guilin 541004, China, and also with the Guangxi Key Lab of Multi-Source Information Mining and Security, Guangxi Normal University, Guilin 541004, China (e-mail: maoyk@stu.gxnu.edu.cn; liujiafei@gxnu.edu.cn; wjlhappy@gxnu.edu.cn; ligaoshi@gxnu.edu.cn).

Sun-Yuan Hsieh is with the Department of Computer Science and Information Engineering, National Cheng Kung University, Tainan 701, Taiwan (e-mail: hsiehsy@mail.ncku.edu.tw).

Digital Object Identifier 10.1109/TR.2025.3638418

the cyclic diagnosability of the regular networks and compared it with other kinds of conditional diagnosabilities. The majority of studies have focused on single-condition diagnosability metrics. These metrics are based on independent topological conditions, including g-good-neighbor, h-extra, and r-component conditions. For instance, the h-extra conditional diagnosability of twisted hypercubes is $(h+1)n-\frac{1}{2}h(h+1)$ for $n \geq 5, 0 \leq h \leq \frac{n-1}{4}$ under the MM$*$ model [7]. Zhang et al. [8] showed that the g-good-neighbor conditional diagnosability of DQcube is $2^g(n+2-g)-1$ and the $(r+1)$-component conditional diagnosability of DQcube is $-\frac{1}{2}r^2+(n-\frac{1}{2})r+n+1$ for $1 \leq r \leq n-2$ under the PMC and MM$*$ models. Liu et al. [26] investigated the g-good-neighbor conditional connectivity and diagnosability on circulant-based recursive networks. Liu et al. [9] explored the r-component conditional diagnosability of the compound networks based on the hypercube. Furthermore, the study revealed the relationship between r-component conditional diagnosability and r-component conditional connectivity. Huang et al. [10] derived that the r-component conditional diagnosability of hierarchical cubic networks is $rn-\frac{1}{2}(r-1)r+1$ for $n \geq 2, 1 \leq r \leq n-1$ under the PMC and MM$*$ models. Sardroud and Ghasemi [11] showed that the g-good-neighbor conditional diagnosability of triangle-free graphs under the MM$*$ and PMC models.

While single-condition diagnosability metrics focus on an isolated aspect of network resilience, they exhibit distinct characteristics: the r-component condition emphasizes global partitioning of the network, the h-extra condition prioritizes the size of the remaining network and the g-good-neighbor condition highlights the local connectivity of nodes. However, in real scenarios, failures often disrupt both the global and local levels of network connectivity simultaneously. Consequently, there has been a growing body of research on diagnosability metrics under combined conditions, aiming to provide more comprehensive and realistic evaluations of network resilience. Zhuo et al. [24] proposed a general approach to determine the non-inclusive h-extra diagnosability of regular graphs. Liao et al. [13] investigated the h-extra r-component connectivity and diagnosability of the bubble sort network. Liu et al. [14] provided a theoretical derivation of the h-extra r-component connectivity (for $h=1, r=2,3,4$) for the star network, and developed a fault diagnostic algorithm to detect faulty nodes.

However, despite these significant advancements, the research on diagnosability under multiple combined conditions still awaits further in-depth exploration. In this study, we address the research gap by analyzing the g-good-neighbor r-component diagnosability of hypercube networks under the PMC and MM$*$ models. Our principal contributions are outlined below:

1) We propose a novel diagnosis measurement, the g-good-neighbor r-component diagnosability, denoted by $D_{g,r}(G)$, which characterizes the local connectivity and the global partitioning of the network.
2) We formally establish the 2-good-neighbor 2-component diagnosability of n-dimensional hypercube Q_n under the PMC and MM$*$ diagnostic models, proving that $D_{2,2}(Q_n)=8n-21$ holds for $n \geq 24$. These results extend classical diagnosability theory by integrating topological resilience metrics with combinatorial fault tolerance analysis, providing a more nuanced evaluation of network survivability under hybrid failure scenarios.
3) We present two multistage fault diagnosis algorithms (TSFD-PMC and FSFD-MM$*$) tailored for regular network architectures. These algorithms leverage model-specific diagnostic principles—mutual testing verification for PMC and comparison-based diagnosis for MM$*$—to achieve polynomial time complexity in hypercube networks. The design philosophy prioritizes adaptive fault localization over exhaustive testing, enabling scalable deployment in large-scale systems.
4) Extensive simulations on Q_n $(n=10 \sim 13)$ validate the algorithms' efficacy. Under moderate fault densities ($\leq 20\%$), two algorithms achieve approximately 100% true positive rate (TPR) with negligible false positive rate (FPR). Even at extreme fault levels (approaching 50%), TSFD-PMC sustains TPR $> 99.5\%$ while FSFD-MM$*$ maintains TPR $> 98.7\%$, demonstrating robustness against correlated failures.

Paper Organization: Section II formalizes notations, diagnostic models (PMC/MM$*$), and structure and properties of hypercube Q_n. Section III establishes the 2-good-neighbor 2-component diagnosability of Q_n under the PMC and MM$*$ models. Section IV details two fault diagnosis algorithms. Section V validates performance of algorithms through hypercube simulations. Section VI synthesizes findings and future directions.

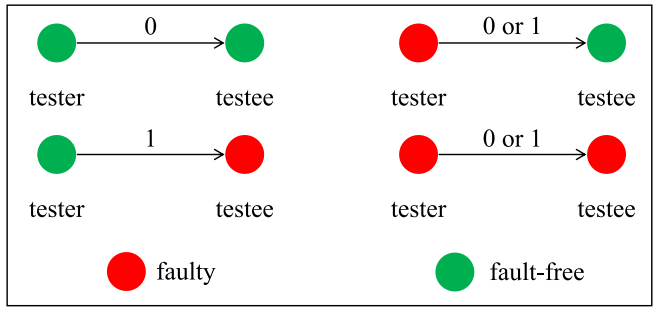

Fig. 1. Testing rules of the PMC model.

II. Preliminaries

Now, we introduce the essential notations, definitions, diagnostic models, and hypercube that are relevant to the following content. The key notations and their explanations used throughout this article are summarized in Table I.

Under the PMC model, adjacent node pairs (u,w) in the network execute reciprocal tests. All test results $\sigma(u,w)$ are aggregated into a syndrome set σ, with the accuracy of each result determined by the operational status of the tester. To facilitate comprehension of the PMC testing protocol, refer to Fig. 1.

Definition 1: [1] The PMC model defines diagnostic rules as follows:

TABLE I
NOTATIONS AND EXPLANATIONS

Notation	Explanation
$G=(V(G),E(G))$	An undirected graph with node set $V(G)$ and edge set $E(G)$
$\lvert V(G)\rvert$	Total nodes count of G
$\lvert E(G)\rvert$	Total edges count of G
(u,w)	Edge between adjacent nodes u and w
$G-S$	Subgraph of G formed by removing node subset S and all edges linked to S
$N_G(u)$	Neighborhood of node u: $\{w\in V(G)\mid (u,w)\in E(G)\}$
$\deg_G(u)$	Degree of u: $\lvert N_G(u)\rvert$
$N_G[u]$	$N_G(u)\cup\{u\}$
$N_G(S)$	Adjacent nodes of set S: $\left(\bigcup_{u\in S}N_G(u)\right)-S$
P_n	A path in graph G is an ordered sequence of n distinct nodes $v_1,v_2,\ldots,v_n$ such that $(v_j,v_{j+1})\in E(G)$ for $j=1,2,\ldots,n$, denoted as $v_1v_2\cdots v_n$
C_n	A cycle in graph G is a closed path consisting of n distinct nodes $v_1,v_2,\ldots,v_n$ and n edges, where $(v_j,v_{j+1})\in E(G)$ for $j=1,2,\ldots,n$ and $(v_n,v_1)\in E(G)$, denoted as $v_1v_2\cdots v_nv_1$
$g(G)$	Shortest cycle length in graph G, i.e., the girth of G
$F_1\triangle F_2$	$(F_1-F_2)\cup(F_2-F_1)$

1) If u is fault-free, $\sigma(u,w)$ is reliable:

$$\sigma(u,w)=\begin{cases}0 & \text{w is fault-free}\\ 1 & \text{w is faulty.}\end{cases}$$

2) If u is faulty, $\sigma(u,w)$ becomes unreliable and may randomly yield 0 or 1, making it impossible to distinguish the status of testee w.

Under the MM$*$ model, each node v tests all pairs of its adjacent neighbors (u,w). All test outcomes $\sigma(u,w)_v$ form a syndrome set σ. The reliability of test outcomes depends on the tester's status (see Fig. 2).

Definition 2: [3] The MM$*$ model defines diagnostic rules as follows:

1) If v is fault-free, $\sigma(u,w)_v$ is reliable:

$$\sigma(u,w)_v=\begin{cases}0 & \text{u and w are fault-free}\\ 1 & \text{either u or w is faulty.}\end{cases}$$

2) If v is faulty, $\sigma(u,w)_v$ becomes unreliable and may randomly yield 0 or 1, making the status of tested nodes u and w undetermined.

We now introduce Lemmas 1 and 2, which outline the conditions for differentiating two distinct node sets F_1 and F_2 under the PMC and MM$*$ models, respectively.

Lemma 1: [1] For PMC model, two distinct node subsets F_1 and F_2 are distinguishable if there are two nodes u and v, with $u\in V(G)-(F_1\cup F_2)$, such that u and v are connected by an edge and v belongs to either F_1-F_2 or F_2-F_1 (see Fig. 3).

Lemma 2: [3] For MM$*$ model, two distinct node subsets F_1 and F_2 are distinguishable if there are three nodes u, v and w, with $u\in V(G)-(F_1\cup F_2)$, such that edges (u,v) and (u,w) meet one of these conditions (see Fig. 4):

1) Both v and w are in F_1-F_2;
2) Both v and w are in F_2-F_1;
3) $v\in V(G)-(F_1\cup F_2)$ and $w\in(F_1-F_2)\cup(F_2-F_1)$.

Now, we review the definition of hypercube and its necessary properties, along with lemmas.

Definition 3: [16] An n-dimensional hypercube Q_n is defined as a graph $Q_n=(V(Q_n),E(Q_n))$ (see Fig. 5) such that:

1) The node set $V(Q_n)=\{p_1p_2\cdots p_n|p_j\in\{0,1\},j=1,2,\ldots,n\}$;

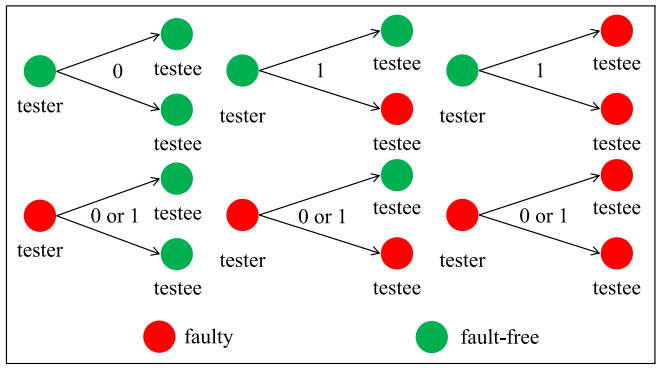

Fig. 2. Testing rules of the MM$*$ model.

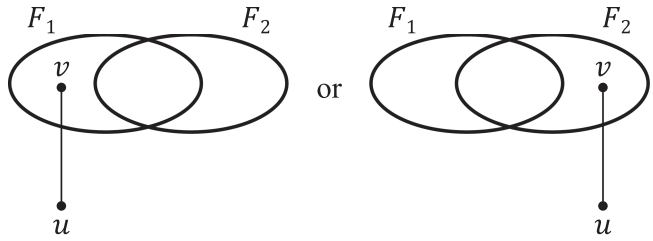

Fig. 3. Distinguishable pair (F_1,F_2) of PMC model.

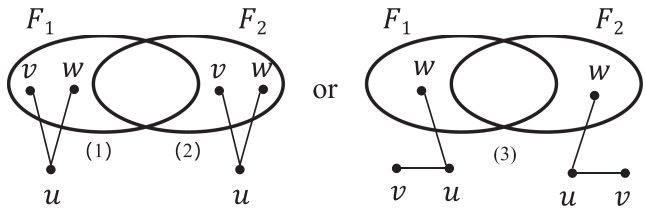

Fig. 4. Distinguishable pair (F_1,F_2) of MM$*$ model.

2) The edge set $E(Q_n)=\{(p,q)|p,q\in V(Q_n),p=p_1p_2\cdots p_n,q=q_1q_2\cdots q_n,\sum_{j=1}^{n}|p_j-q_j|=1\}$.

Proposition 1: [15], [16] Q_n possesses some fundamental properties:

1) Q_n is n-regular with 2^n nodes and $n2^{n-1}$ edges;
2) $g(Q_n)=4$ $(n\geq 2)$;
3) Q_n is bipartite and contains no odd cycle;

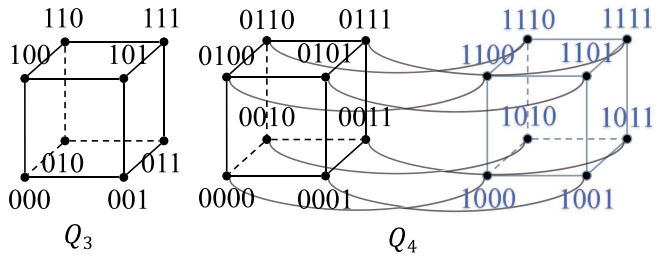

Fig. 5. Illustration of Q_n for $n = 3, 4$.

4) In Q_n, two different nodes either share no common neighbor or share exactly two common neighbors.

Definition 4: [12] For an undirected graph $G = (V(G), E(G))$, a node subset S of $V(G)$ is termed a g-good-neighbor r-component faulty set when $G - S$ comprises no less than r components and each node of $G - S$ contains no less than g good neighbors.

Definition 5: [12] For an undirected graph $G = (V(G), E(G))$, a node subset S of $V(G)$ is referred to as a g-good-neighbor r-component node cut of G provided that S is a g-good-neighbor r-component faulty set. The g-good-neighbor r-component connectivity of G, denoted by $GCC_{g,r}(G)$, is defined to be the smallest size of these node cuts.

Building upon the aforementioned definitions of conditional connectivity, we propose a novel concept, the g-good-neighbor r-component diagnosability.

Definition 6: For an undirected graph $G = (V(G), E(G))$, G is referred to be g-good-neighbor r-component t-diagnosable if, for any two distinct g-good-neighbor r-component fault sets S_1, S_2 of $V(G)$ with $|S_1| \leq t$ and $|S_2| \leq t$, the pair (S_1, S_2) is distinguishable. The greatest value of t is termed the g-good-neighbor r-component diagnosability of G, signified by $D_{g,r}(G)$.

III. Main Results

In this part, we present the theoretical proof of $D_{2,2}(Q_n)$ under two models.

Lemma 3: [12] For Q_n, its 2-good-neighbor 3-component connectivity $GCC_{2,3}(Q_n) = 8n - 24$ for $n \geq 11$.

Lemma 4: [12] Let C_a and C_b be two 4-cycles in the hypercube Q_n. If $N_{Q_n}(V(C_a)) \cap V(C_b) = \emptyset$ and $N_{Q_n}(V(C_b)) \cap V(C_a) = \emptyset$, then $|N_{Q_n}(V(C_a)) \cap N_{Q_n}(V(C_b))| \leq 8$.

Lemma 5: [25] When $n \geq 4$ and $1 \leq x \leq n-1$, let a subset S of $V(Q_n)$ with $|S|$ not exceeding $xn - \frac{(x-1)(x+2)}{2} - 1$, $Q_n - S$ either has only one connected component or is composed of a large component and several small components, each with no more than $x - 1$ nodes.

Theorem 1: For PMC model, $D_{2,2}(Q_n) \leq 8n - 21$ for $n \geq 10$.

Proof: Let $Z_1 = x_1x_2x_3x_4x_1$ and $Z_2 = y_1y_2y_3y_4y_1$ be two 4-cycles in Q_n, where $x_1 = 00010\cdots00$, $x_2 = 00000\cdots00$, $x_3 = 00100\cdots00$, $x_4 = 00110\cdots00$, $y_1 = 11010\cdots00$, $y_2 = 11000\cdots00$, $y_3 = 11100\cdots00$, $y_4 = 11110\cdots00$. For each $i \in \{1, 2, 3, 4\}$, x_i and y_i share exactly two common neighbors: $c_1 = 10010\cdots00$, $c_2 = 01010\cdots00$ for $i = 1$; $c_3 = 10000\cdots00$, $c_4 = 01000\cdots00$ for $i = 2$; $c_5 = 10100\cdots00$, $c_6 = 01100\cdots00$ for $i = 3$; $c_7 = 10110\cdots00$, $c_8 = 01110\cdots00$ for $i = 4$. Therefore, Z_1 and Z_2 have exactly eight common neighbors. Define node set $X = V(Z_1) \cup V(Z_2)$, $F_1 = N_{Q_n}(X)$, and $F_2 = F_1 \cup V(Z_1)$. Then $F_1 \triangle F_2 = V(Z_1)$ (see Fig. 6). Since Q_n is n-regular, we have $|F_1| = 8(n-2) - 8 = 8n - 24$ and $|F_2| = |F_1| + |V(Z_1)| = 8n - 20$. For $n \geq 10$, it follows that $|V(Q_n)| - |F_2 \cup V(Z_2)| \geq 2^n - (8n - 20) - 4 \geq 4$. Thus, $Q_n - F_2$ contains at least two components.

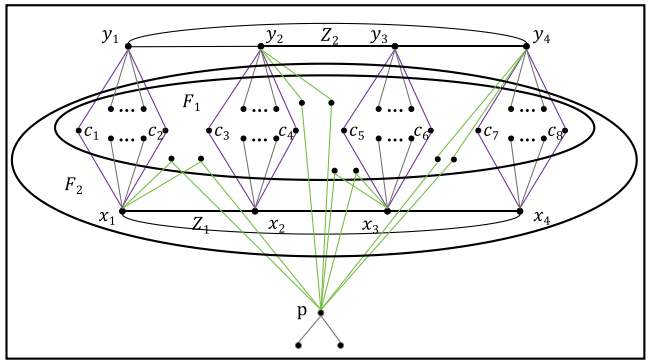

Fig. 6. Indistinguishable pair (F_1, F_2).

Now, we demonstrate that every node in $V(Q_n) - (F_2 \cup V(Z_2))$ possesses no less than two good neighbors. Let node $p \in V(Q_n) - (F_2 \cup V(Z_2))$. If p and y_1 share two neighbors in $N_{Q_n}(X)$, there is no common neighbor between p and y_2 (or y_4), otherwise, they would form an odd cycle, contradicting Proposition 1(3). Meanwhile, p and y_3 share at most two neighbors in $N_{Q_n}(X)$. This implies that $|N_{Q_n}(p) \cap N_{Q_n}(V(Z_2))| \leq 4$ and similarly $|N_{Q_n}(p) \cap N_{Q_n}(V(Z_1))| \leq 4$. When $n \geq 10$, $deg_{Q_n - F_2}(p) \geq n - |N_{Q_n}(p) \cap N_{Q_n}(V(Z_1) \cup V(Z_2))| \geq n - 8 \geq 2$. So every node in $V(Q_n) - (F_2 \cup V(Z_2))$ has no less than two good neighbors. This means that F_2 qualifies as a 2-good-neighbor 2-component node cut. By the similar derivation method, we can confirm that F_1 also satisfies the criteria for such a node cut. Given that there are no connecting edges between $F_1 \triangle F_2$ and $V(Q_n) - (F_2 \cup V(Z_2))$, it follows from Lemma 1 that F_1 and F_2 cannot be distinguished. As $|F_1| \leq 8n - 20$ and $|F_2| \leq 8n - 20$, Q_n is not 2-good-neighbor 2-component $(8n - 20)$-diagnosable. Therefore, $D_{2,2}(Q_n) \leq 8n - 21$ for $n \geq 10$. □

Theorem 2: For PMC model, $D_{2,2}(Q_n) \geq 8n - 21$ for $n \geq 24$.

Proof: We suppose, to the contrary, that $D_{2,2}(Q_n) \leq 8n - 22$. Then by Definition 6, there exist two distinct 2-good-neighbor 2-component node cuts, F_1 and F_2, which are subsets of $V(Q_n)$, with $|F_1|, |F_2| \leq 8n - 21$, and they cannot be distinguished. Assume that $F_2 - F_1 \neq \emptyset$. By Lemma 5, we have $8n - 21 \leq 9n - 45$ for $n \geq 24$. It means that $Q_n - F_2$ contains a large component denoted as A and a residual set B of small components whose combined cardinality is at most eight. Since F_2 is a 2-good-neighbor 2-component node cut, each node in any component of $Q_n - F_2$ has at least two good neighbors within that component; hence each component has at least four nodes.

Consequently, $4 \leq |V(B)| \leq 8$. We have $|V(A)| = |V(Q_n)| - |F_2| - |V(B)| \geq 2^n - (8n-21) - 8 \geq 2^n - 8n + 13$. Since $n \geq 24$, $|V(A)| - |F_1| \geq 2^n - 8n + 13 - (8n-21) \geq 2^n - 16n + 34 > 0$. As F_1 and F_2 cannot be distinguished, the subgraph $V(Q_n) - (F_1 \cup F_2)$ is disconnected to $F_1 \triangle F_2$ due to Lemma 1. Now, consider two cases according to the relationship of the two subsets.

Case 1: $F_1 \subset F_2$, i.e., $F_1 \triangle F_2 = F_2 - F_1$

Since F_2 is a 2-good-neighbor 2-component node cut, $Q_n - F_2$ contains at least two components. As F_1 is a 2-good-neighbor 2-component node cut, it follows that $|F_2 - F_1| \geq 4$ and each node in $F_2 - F_1$ has two good neighbors. Consequently, F_1 is a 2-good-neighbor 3-component node cut. By Lemma 3, $|F_1| \geq GCC_{2,3}(Q_n) = 8n - 24$. Therefore, $|F_2| = |F_2 - F_1| + |F_1| \geq 4 + (8n-24) = 8n - 20$, contradicting the assumption $|F_2| \leq 8n - 21$.

Case 2: $F_2 - F_1 \neq \emptyset$ and $F_1 - F_2 \neq \emptyset$

Noting that F_2 is a 2-good-neighbor 2-component node cut and the subgraph $V(Q_n) - (F_1 \cup F_2)$ is disconnected to $F_1 - F_2$, $F_1 - F_2$ is a small component of B and its cardinality is no less than 4. Similarly, $|F_2 - F_1| \geq 4$. Obviously, $|F_1 \cap F_2| = |F_2| - |F_2 - F_1| \leq 8n - 25 \leq 9n - 45$ for $n \geq 24$. By Lemma 5, $Q_n - F_1 \cap F_2$ contains a large component and some small components having no more than eight nodes. It follows that $|F_1 - F_2| + |F_2 - F_1| \leq 8$. Then, we have $|F_1 - F_2| = 4$ and $|F_2 - F_1| = 4$. Hence, $F_1 - F_2$ is a 4-cycle denoted by $Z_3 = abcda$ and $F_2 - F_1$ is also a 4-cycle denoted by $Z_4 = efghe$.

Now, we consider the scenario where Z_3 is connected to Z_4. Let $Z_5 = Z_3 \cup Z_4$. Then, all neighbors of Z_5 are contained in $F_1 \cap F_2$. If there exists a connecting edge between Z_3 and Z_4 (e.g., $(a,e) \in E(Z_5)$), the number of neighbors of Z_5 is $|N(Z_5)| \geq 8n - 22$. If there exist two direct connecting edges (e.g., edges $(a,e),(b,f) \in E(Z_5)$), $|N(Z_5)| \geq 8n - 20$. If there exist three direct connecting edges (e.g., edges $(a,e),(b,f),(c,g) \in E(Z_5)$), the neighbor count of Z_5 is $|N(Z_5)| \geq 8n - 22$. If there exist four direct connecting edges, Z_5 exactly forms a subgraph isomorphic to Q_3 (see Fig. 7), and its number of neighbors is $|N(Z_5)| = 8(n-3) = 8n - 24$. Notably, Z_3 and Z_4 share at most four connecting edges; otherwise, this would contradict the structural properties of the hypercube [Proposition 1(3),(4)]. Thus, the number of neighbors of Z_5 is at least $8n - 24$, i.e., $|F_1 \cap F_2| \geq 8n - 24$. Thus, the number of neighbors of Z_5 is at least $8n - 24$, i.e., $|F_1 \cap F_2| \geq 8n - 24$. Thus, $|F_2| = |F_2 - F_1| + |F_1 \cap F_2| \geq 4 + (8n-24) = 8n - 20$, contradicting the constraint that $|F_2| \leq 8n - 21$.

If Z_3 and Z_4 are disconnected, $F_1 \cap F_2$ is a 2-good-neighbor 3-component node cut. By Lemma 3, $|F_1 \cap F_2| \geq GCC_{2,3}(Q_n) = 8n - 24$. Then $|F_2| = |F_2 - F_1| + |F_1 \cap F_2| \geq 8n - 20$, contradicting the assumption $|F_2| \leq 8n - 21$. So $D_{2,2}(Q_n) \geq 8n - 21$ under the PMC model for $n \geq 24$. □

Theorem 3 can be directly derived from the two aforementioned Theorems 1 and 2.

Theorem 3: For PMC model, $D_{2,2}(Q_n) = 8n - 21$ for $n \geq 24$.

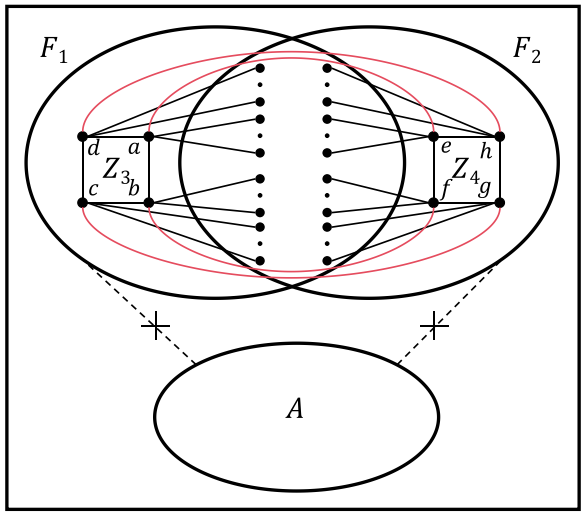

Fig. 7. Illustration of the connections between Z_3 and Z_4.

Next, we propose the theoretical derivations regarding $D_{2,2}(Q_n)$ for the MM$*$ model.

Theorem 4: For MM$*$ model, $D_{2,2}(Q_n) \leq 8n - 21$ for $n \geq 10$.

Proof: The upper bound of the 2-good-neighbor 2-component diagnosability of hypercube can be determined by using the same technical route as Theorem 1. Therefore, $D_{2,2}(Q_n) \leq 8n - 21$. □

Theorem 5: For MM$*$ model, $D_{2,2}(Q_n) \geq 8n - 21$ for $n \geq 24$.

Proof: We suppose, to the contrary, that $D_{2,2}(Q_n) \leq 8n - 22$. Based on Definition 6, within $V(Q_n)$, there exist two distinct 2-good-neighbor 2-component node cuts F_1 and F_2. Each of them has a cardinality of no more than $8n - 21$, and they cannot be distinguished under the MM$*$ model. Without loss of generality, let $F_2 - F_1 \neq \emptyset$. Obviously, $|V(Q_n) - (F_1 \cup F_2)| \geq 2^n - 2(8n-21) > 0$ for $n \geq 24$. Based on the relationship of F_1 and F_2, two possibilities can be discussed as below.

Case 1: $F_1 \subset F_2$, i.e., $F_1 \triangle F_2 = F_2 - F_1$

Since F_2 is a 2-good-neighbor 2-component node cut, $Q_n - F_2$ contains at least two connected components $S_1, S_2, \ldots, S_m$ with $|S_i| \geq 4$ for $m \geq 2$ and each node $v \in S_i$ satisfies $\deg_{S_i}(v) \geq 2$ for $1 \leq i \leq m$. As F_1 and F_2 are distinct, we have $F_2 - F_1 \neq \emptyset$. Let node $q \in F_2 - F_1$. As F_1 is a 2-good-neighbor 2-component node cut, q has at least two neighbors in $Q_n - F_1$. Suppose q is adjacent to some node $l \in S_i$. Obviously, l has at least two neighbors other than q within S_i. Hence, $l \in V(Q_n) - (F_1 \cup F_2)$ is adjacent to $q \in F_2 - F_1$, and has no less than two neighbors in $V(Q_n) - (F_1 \cup F_2)$. Hence, F_1 and F_2 are distinguishable by Lemma 2(3), which contradicts that F_1 and F_2 cannot be distinguished. Consequently, $F_2 - F_1$ is disconnected to $Q_n - F_2$, which implies that each node of $F_2 - F_1$ has no less than two neighbors in $F_2 - F_1$ and its cardinality is no more than 4. Therefore, F_1 is a 2-good-neighbor 3-component node cut. It follows that $|F_1| \geq GCC_{2,3}(Q_n) = 8n - 24$ for $n \geq 11$ by Lemma 3. And $|F_2| = |F_2 - F_1| +$

$|F_1| \geq 4 + (8n - 24) = 8n - 20$, contradicting the assumption $|F_2| \leq 8n - 21$.

Case 2: $F_1 - F_2 \neq \emptyset$ and $F_2 - F_1 \neq \emptyset$

Since F_1 is a 2-good-neighbor 2-component node cut, $Q_n - F_1$ contains at least two connected components $S_1, S_2, \ldots, S_m$ with $|S_i| \geq 4$ for $m \geq 2$ and each node $v \in S_i$ satisfies $\deg_{S_i}(v) \geq 2$ for $1 \leq i \leq m$. Let node $w \in V(Q_n) - (F_1 \cup F_2)$ and $w \in S_i$. If w has at least two neighbors of $F_2 - F_1$, F_1 and F_2 are distinguishable by Lemma 2(1), contradicting the constraint that they cannot be distinguished. If w has exactly one good neighbor in $F_2 - F_1$ and other good neighbors in $Q_n - F_1 \cup F_2$, it implies that F_1 and F_2 are distinguishable by Lemma 2(3), which contradicts that they cannot be distinguished. Consequently, all neighbors of w are in $V(Q_n) - (F_1 \cup F_2)$, i.e., $S_i \subset V(Q_n) - (F_1 \cup F_2)$. Due to w is arbitrary, the subgraph $V(Q_n) - (F_1 \cup F_2)$ is disconnected to $F_2 - F_1$. Thus, for each node of $F_2 - F_1$, its all neighbors are in $F_2 - F_1$, and the cardinality of $F_2 - F_1$ is more than 4. Similarly, there is no edge between $V(Q_n) - (F_1 \cup F_2)$ and $F_1 - F_2$, and $|F_1 - F_2| \geq 4$. All neighbors of $F_1 \triangle F_2$ belong to $F_1 \cap F_2$. In addition, we have $|F_1 \cap F_2| = |F_2| - |F_2 - F_1| \leq 8n - 21 - 4 = 8n - 25 \leq 8n - 21 \leq 9n - 45$ for $n \geq 24$. By Lemma 5, $Q_n - F_1 \cap F_2$ contains some small components having no more than eight nodes. It follows that $|F_1 - F_2| + |F_2 - F_1| \leq 8$. Obviously, $|F_1 - F_2|$ and $|F_2 - F_1|$ each have a cardinality of 4. If $F_1 - F_2$ is connected to $F_2 - F_1$, similar to Theorem 2, we have $|F_1 \cap F_2| \geq |N_{Q_n}(F_1 \triangle F_2)| \geq 8n - 24$ and $|F_2| = |F_2 - F_1| + |F_1 \cap F_2| \geq 8n - 20$, contradicting the constraint that $|F_2| \leq 8n - 21$. When $F_1 - F_2$ is disconnected to $F_2 - F_1$, $F_1 \cap F_2$ is a 2-good-neighbor 3-component node cut. By Lemma 3, $|F_1 \cap F_2| \geq GCC_{2,3}(Q_n) = 8n - 24$. Therefore, $|F_2| = |F_2 - F_1| + |F_1 \cap F_2| \geq 8n - 20$, contradicting the assumption $|F_2| \leq 8n - 21$. So we conclude that $D_{2,2}(Q_n) \geq 8n - 21$ for $n \geq 24$. The proof is complete. □

Theorem 6 is directly derived from the two aforementioned Theorems 4 and 5.

Theorem 6: For MM$*$ model, $D_{2,2}(Q_n) = 8n - 21$ for $n \geq 24$.

IV. Algorithms

Within this section, we put forward two novel fault diagnosis algorithms based on the theoretical features of the PMC/MM$*$ models, which are intended to enable efficient and timely diagnosis of faulty networks.

Specifically, motivated by the test characteristic of the PMC model (Definition 1), we introduce Algorithm 1, namely Two-Stage Fault Diagnosis algorithm under the PMC model (TSFD-PMC) to achieve efficient fault detection in interconnection networks. The algorithm's core mechanism is rooted in the fundamental PMC diagnostic rule: if $\sigma(v, u) = 0$ and $\sigma(u, v) = 1$, this indicates that v must be faulty. This principle enables TSFD-PMC to integrate direct fault detection with statistical inference, optimizing both diagnostic speed and accuracy.

Given a regular graph G and a syndrome σ generated by m faulty nodes under the testing PMC model, the algorithm

Algorithm 1: Two-Stage Fault Diagnosis Algorithm.

Require: Graph $G(V(G), E(G))$, Syndrome σ
Ensure: Diagnosed faulty set F, Diagnosed fault-free set FF

1: **Initialize:**
2: $F \leftarrow \emptyset, FF \leftarrow \emptyset$ ▷ Empty diagnosis set
3: $C(v) \leftarrow 0, \forall v \in V(G)$ ▷ Initialize counters for all nodes
4: **Phase 1: Direct Diagnosis**
5: **for** each node $v \in V(G)$ **do** ▷ Traverse all nodes
6: **for** each neighbor $u \in N(v)$ **do** ▷ Check neighbors
7: **if** $\sigma(v, u) = 0$ **then** ▷ $\sigma(v, u)$ means v test u
8: **if** $\sigma(u, v) = 1$ **then**
9: $F \leftarrow F \cup \{v\}$ ▷ Confirm v is faulty
10: **end if**
11: **else**
12: $C(v) \leftarrow C(v) + 1$ ▷ Increment counters
13: $C(u) \leftarrow C(u) + 1$
14: **end if**
15: **end for**
16: **end for**
17: $F_{\text{dir}} \leftarrow F$ ▷ Directly diagnosed faulty nodes
18: **Phase 2: Counter-based Expanding Diagnosis**
19: $r \leftarrow \lfloor |F_{\text{dir}}|/2 \rfloor$ ▷ Select possible faulty nodes
20: $S \leftarrow V(G)$ ▷ S is an ordered sequence of all nodes
21: $S \leftarrow \text{sort}(S, \text{by } C(v) \text{ descending})$ ▷ Sort all nodes by counter value descending
22: $F_{\text{ex}} \leftarrow \{S_1, S_2, \ldots, S_r\} - F_{\text{dir}}$ ▷ Select top r nodes, $S_1, S_2, \ldots, S_r$, excluding direct faulty nodes
23: $F \leftarrow F_{\text{dir}} \cup F_{\text{ex}}$ ▷ Add expanding faulty nodes
24: $FF \leftarrow V(G) - F$ ▷ All remaining nodes are fault-free
26: **return** F, FF

TSFD-PMC identifies the fault set $F \subset V(G)$ and fault-free set $FF \subset V(G)$ through the following phases:

1) *Initialization (Lines 1-3):* Establishes two empty sets F and FF to keep track of faulty and fault-free nodes, respectively; and initializes counters $C(v)$ to represent the number of times that the symptom result is 1 when node v is taken as the tester. The initialization phase prepares the data structures for the subsequent analysis. For the initialization, its time complexity is $\mathcal{O}(1)$.
2) *Direct Diagnosis (Lines 4-17):* This phase employs a dual-loop structure to systematically identify faulty nodes: The outer loop traverses each node $v \in V(G)$, while the inner loop examines each neighbor $u \in N(v)$. During this phase, we analyze test pairs $(\sigma(v, u), \sigma(u, v))$ according to PMC principles: When $\sigma(v, u) = 0$, we verify the reciprocal test. If $\sigma(u, v) = 1$, we confirm v as faulty and add it into F. When $\sigma(v, u) = 1$, both counters of v and u are incremented by 1. After traversing all nodes and their neighbors, the set of directly diagnosed faulty nodes is recorded as F_{dir}. This stage is carried out in $\mathcal{O}(Nn)$ time, where $N = |V(G)|$ and n represents the regular degree

of the graph, ensuring all node pairs are evaluated before proceeding to statistical inference.

3) *Counter-based Expanding Diagnosis (Lines 18-25):* This phase expands the faulty set using counter values. First, r is calculated as $\lfloor |F_{\text{dir}}|/2 \rfloor$. The choice of $r = \lfloor |F_{\text{dir}}|/2 \rfloor$ is dictated by the outcome of Direct Diagnosis phase. After the Direct Diagnosis phase terminates, the vast majority of faulty nodes—whose counters $C(v)$ are exceptionally high—have already been identified and collected into F_{dir}. Empirical observation across multiple runs shows that when r is set to $\lfloor |F_{\text{dir}}|/2 \rfloor$, the top r nodes ranked by $C(v)$ still contain some undetermined faulty nodes, while remaining sufficiently small to avoid labeling an excessive number of fault-free nodes as faulty. Larger values of r noticeably increase the FPR; the adopted value therefore offers a pragmatic balance between detecting residual faulty nodes and keeping misdiagnosis low. Then, all nodes in $V(G)$ are sorted in descending order of their counter values $C(v)$ to form the sequence S. The top r nodes in S, excluding those already in F_{dir}, form the expanding faulty set F_{ex}. The final faulty set F is the union of F_{dir} and F_{ex}, and the fault-free set FF is $V(G) - F$. Finally, return the final results F and FF. The time complexity of this phase is determined by the sorting operation, with a time complexity of $O(NlogN)$.

The TSFD-PMC's complexity of $\mathcal{O}(NlogN)$ stems from its efficient mechanism, making it particularly suitable for large-scale HPC systems.

Building upon the comparative testing principles of the MM$*$ model (Definition 2), we propose Algorithm 2 Four-Stage Fault Diagnosis under the MM$*$ Model (FSFD-MM$*$). In contrast to the pairwise testing mechanism of the PMC model, FSFD-MM$*$ leverages neighbor-pair analysis for diagnostic inference. For a fault-free tester v, the following diagnostic rules apply: if $\sigma(u,w)_v = 0$, we confirm u and w as fault-free nodes; when $\sigma(u,w)_v = 1$ and one of $\{u,w\}$ is fault-free, the other must be faulty. This comparative testing framework enables simultaneous fault diagnosis and fault-free node validation through dynamic propagation, enabling the algorithm to expand the set of confirmed fault-free nodes iteratively as it identifies faulty nodes.

Similar to TSFD-PMC, the FSFD-MM$*$ algorithm operates on a regular graph G with syndrome σ generated by the MM$*$ framework under m faulty nodes. The algorithm confirms F and FF through the following phases:

1) *Initialization (Lines 1-3):* Initialize two empty diagnosis sets F and FF. Executed in $\mathcal{O}(1)$ time, it prepares the required data structures for subsequent analysis.
2) *Neighbor-Pair Analysis (Lines 4-12):* For each node v, systematically analyze its all neighbor pairs (u,w). When $\sigma(u,w)_v = 1$, the counters $C(u)$ and $C(w)$ are incremented by 1. This procedure, which runs in $\mathcal{O}(Nn^2)$ time, identifies potential fault candidates through comparative tests.
3) *Initial Filtering (Lines 13-16):* Identify initial fault-free nodes $FF \leftarrow \{v \in V(G) \mid C(v) \leq C_n^2\}$. The threshold $C_n^2 = \frac{n(n-1)}{2}$ is chosen for the following reasons. After Neighbor-Pair Analysis phase, every node v has been examined as one endpoint of all ordered test pairs; hence the maximum possible counter value $C(v)$ is $n(n-1)$, i.e., A_n^2. Empirical evidence shows a clear bimodal distribution of $C(v)$: When faulty nodes are sparse, a faulty node surrounded by fault-free nodes attains $C(v) = A_n^2$, whereas a fault-free node encompassed by other fault-free nodes yields $C(v) = 0$. As the fault density increases, fault-free nodes drift away from $C(v) = 0$ and faulty nodes from $C(v) = A_n^2$, however, across thousands of runs the mid-point $\frac{1}{2}A_n^2 = C_n^2$ remains the stable crossover: counters of fault-free rarely exceed C_n^2, whereas faulty ones rarely fall below it. Consequently, the initial fault-free set $FF \leftarrow \{v \in V(G) \mid C(v) \leq C_n^2\}$ is extracted at this boundary. Despite a slight risk of misdiagnosis, the overall fault-identification rate remains virtually unaffected. Then, take these nodes of FF into a processing queue Q, and define undecided nodes $U \leftarrow V(G) - F \cup FF$. This phase runs in $\mathcal{O}(N)$ time.
4) *Dynamic Propagation (Lines 17-35):* The core innovation of FSFD-MM$*$ lies in its queue-driven propagation mechanism. The algorithm initializes a processing queue Q with fault-free nodes and iteratively dequeues nodes v to analyze their neighbor pairs (u,w). When $\sigma(u,w)_v = 0$, u and w, which are not already classified, are added into FF and Q for further propagation. When $\sigma(u,w)_v = 1$, w is determined to be faulty and $F \leftarrow F \cup \{w\}$, if u belongs to FF. When node v tests all its neighbor pairs, it is dequeued from the queue Q, and then the next node in Q is processed. The phase continues processing until queue Q becomes empty. Then, update $U \leftarrow V(G) - F \cup FF$. This phase achieves $\mathcal{O}(Nn^2)$ time complexity due to exhaustive neighbor pair analysis.
5) *Residual Resolution (Lines 36-38):* After the preceding phases, the majority of nodes have been classified as faulty or fault-free. If all neighbors of an undecided node $u \in U$ in the previous phase are identified as faulty, it would be classified into the faulty set F. Under realistic fault densities, this situation is rare, so the members of U are predominantly faulty. Consequently, we conservatively classify every node in U as faulty, which introduces only a negligible number of false positives while ensuring that no actual fault is missed. The remaining undecided nodes in U are classified as faulty by setting $F \leftarrow F \cup U$. For this stage, its time complexity is $\mathcal{O}(N)$.

Therefore, the FSFD-MM$*$ algorithm achieves $\mathcal{O}(Nn^2)$ time complexity due to exhaustive neighbor pair comparisons.

V. Simulations

In this section, to ensure reproducibility, we first detail the hardware and software environment in which all experiments were conducted. Table II summarizes the platform configuration and the versions of the core libraries employed throughout this study.

Algorithm 2: Four-Stage Fault Diagnosis Algorithm.

Require: Graph $G(V(G), E(G))$, Syndrome σ
Ensure: Diagnosed faulty set F, Diagnosed fault-free set FF

Initialize:
$F \leftarrow \emptyset, FF \leftarrow \emptyset$ ▷ Empty diagnosis set
$C(v) \leftarrow 0,\ \forall v \in V(G)$ ▷ Initialize counters for all nodes
Phase 1: Neighbor-Pair Analysis
for $\forall v \in V(G)$ **do**
  for each neighbor pair (u, w) of node v **do**
    if $\sigma(u, w)_v = 1$ **then**
      $C(u) \leftarrow C(u) + 1$ ▷ Increment counters
      $C(w) \leftarrow C(w) + 1$
    end if
  end for
end for
Phase 2: Initial Filtering
$FF \leftarrow \{v \in V(G) \mid C(v) \leq C_n^2\}$ ▷ Identify initial FF
Initialize queue $Q \leftarrow FF$ ▷ Load FF into queue
$U \leftarrow V(G) - F \cup FF$ ▷ Unknown nodes
Phase 3: Dynamic Propagation
while $Q \neq \emptyset$ **do**
  $v \leftarrow Q$.dequeue() ▷ Process next fault-free node
  for each neighbor pair (u, w) of node v **do**
    if $\sigma(u, w)_v = 0$ **then**
      for $x \in \{u, w\}$ **do**
        if $x \notin FF$ **then**
$FF \leftarrow FF \cup \{x\}$ ▷ Expand FF
Q.enqueue(x) ▷ Add fault-free node to Q
          end if
        end for
    else if $\sigma(u, w)_v = 1$ **then**
      if $u \in FF$ **then** $F \leftarrow F \cup \{w\}$ ▷ Confirm w as faulty
      else if $w \in FF$ **then** $F \leftarrow F \cup \{u\}$ ▷ Confirm u as faulty
      end if
    end if
  end for
  $U \leftarrow V(G) - F \cup FF$
end while
Phase 4: Residual Resolution
$F \leftarrow F \cup U$ ▷ Classify all remaining nodes as faulty
return F, FF

TABLE II
EXPERIMENTAL SETUP

Environment Parameter	Specification/Version
CPU	Intel i5-13500
Storage	932 GB HDD, 477 GB SSD
RAM	16.0 GB
IDE	PyCharm Community Edition 2024.2.4
Core Libraries	NumPy: 2.3.3; Pandas: 2.3.3; Networks: 3.5

Now, we carry out comprehensive simulations to assess the performance of Algorithms 1 and 2 on hypercube networks. For each dimension, we choose six faulty ratios $\rho = m/N$ ranging from 10% to 60% . All experiments are conducted with 100 trials within the PMC and MM$*$ diagnostic frameworks. Afterward, we present the diagnostic metrics including TPR, accuracy (ACCR), Precision, true negative rate (TNR), and FPR. The definitions of these metrics are as follows.

1) *TPR:* It denotes the ratio of accurately detected faulty nodes to all faulty nodes in total
$$\text{TPR} = \frac{\text{TP}}{\text{TP} + \text{FN}}.$$
2) *ACCR:* It represents the ratio of nodes identified correctly (including both faulty and fault-free ones) to the overall number of nodes
$$\text{ACCR} = \frac{\text{TN} + \text{TP}}{\text{TN} + \text{FP} + \text{FN} + \text{TP}}.$$
3) *Precision:* It signifies the ratio of accurately identified faulty nodes among all nodes predicted as faulty.
$$\text{Precision} = \frac{\text{TP}}{\text{TP} + \text{FP}}.$$
4) *TNR:* It indicates the ratio of nodes correctly diagnosed as fault-free to the entire count of fault-free nodes
$$\text{TNR} = \frac{\text{TN}}{\text{FP} + \text{TN}}.$$
5) *FPR:* It represents the ratio of fault-free nodes incorrectly diagnosed as faulty to the entire set of genuinely fault-free nodes
$$\text{FPR} = \frac{\text{FP}}{\text{FP} + \text{TN}}.$$

Here, the basic metrics are defined below:
1) *True positives (TP):* Correctly identified faulty nodes.
2) *False positives (FP):* Fault-free nodes misclassified as faulty.
3) *True negatives (TN):* Correctly identified fault-free nodes.
4) *False negatives (FN):* Faulty nodes misclassified as fault-free.

TPR is the most critical metric for our algorithms. It is given priority because it directly measures the fundamental capacity of algorithm to precisely detect all faulty nodes within the network: a high TPR ensures that few actual faults are misdiagnosed, which is vital where undetected faulty nodes can propagate errors, disrupt operations, or cause cascading failures in network systems.

The experimental results of TSFD-PMC on hypercube networks, as detailed in Table III and visualized in Fig. 8, reveal that TSFD-PMC maintains TPR $> 99.5\%$ across all tested dimensions ($n = 10 \sim 13$) and fault ratios ($\rho = 10\% \sim 60\%$). Across any fixed dimension, TSFD-PMC shows only a marginal TPR decay as ρ grows: at $n = 10$ the rate slips from 99.99% ($\rho = 10\%$) to 99.52% ($\rho = 60\%$), yet remains above 99.5% —confirming robust fault identification even under the heaviest load. Equally striking is the impact of dimensional scaling on TPR: for any fixed ρ, TPR improves as n increases. At $\rho = 30\%$,

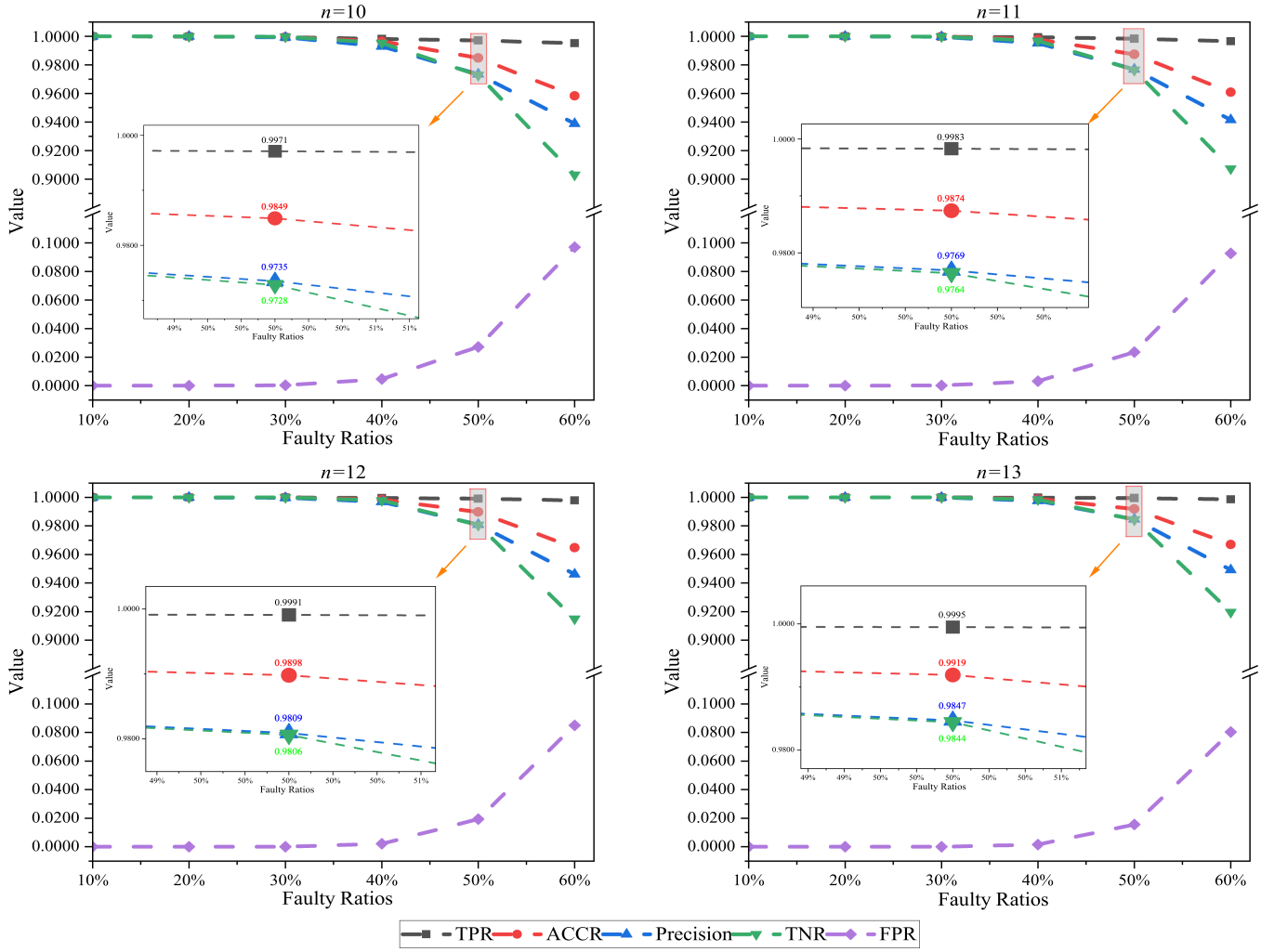

Fig. 8. Performance of TSFD-PMC on hypercube Q_n under varying faulty ratios.

TABLE III
DIAGNOSTIC METRICS OF TSFD-PMC ON HYPERCUBE NETWORKS

Dimension	Faulty Ratios	Diagnostic Metrics				
n	ρ	TPR	ACCR	Precision	TNR	FPR
10	10%	0.9999	1	1	1	0
	20%	0.9998	1	1	1	0
	30%	0.9993	0.9995	0.9992	0.9996	0.0004
	40%	0.9982	0.9965	0.9929	0.9953	0.0047
	50%	0.9971	0.9849	0.9735	0.9728	0.0272
	60%	0.9952	0.9583	0.9389	0.9030	0.0970
11	10%	1	1	1	1	0
	20%	1	1	1	1	0
	30%	0.9996	0.9998	0.9996	0.9998	0.0002
	40%	0.9994	0.9978	0.9952	0.9968	0.0032
	50%	0.9983	0.9874	0.9769	0.9764	0.0236
	60%	0.9965	0.9609	0.9416	0.9074	0.0926
12	10%	1	1	1	1	0
	20%	1	1	1	1	0
	30%	0.9999	0.9999	0.9997	0.9999	0.0001
	40%	0.9995	0.9985	0.9968	0.9978	0.0022
	50%	0.9991	0.9898	0.9809	0.9806	0.0194
	60%	0.9979	0.9647	0.9462	0.9150	0.0850
13	10%	1	1	1	1	0
	20%	1	1	1	1	0
	30%	0.9999	0.9999	0.9999	0.9999	0.0001
	40%	0.9998	0.9989	0.9976	0.9984	0.0016
	50%	0.9995	0.9919	0.9847	0.9844	0.0156
	60%	0.9986	0.9670	0.9491	0.9197	0.0803

for example, TPR rises from 99.93% ($n = 10$) to 99.99% ($n \geq 12$) and stays virtually equal to 100% for $\rho \leq 20\%$ across all dimensions, demonstrating that TSFD-PMC retains near-perfect fault identification capability in large-scale networks. In terms of FPR, TSFD-PMC exhibits similarly favorable behavior. As n increases, FPR decreases consistently for the same ρ. This reduction in false positives further validates the algorithm's enhanced precision in large-scale networks.

FSFD-MM$*$ likewise keeps TPR $> 91\%$ across the full test spectrum (Table IV and Fig. 9). When n is fixed, TPR declines only gradually as ρ increases: for $n = 10$, TPR stays at 100% up to $\rho = 30\%$, then slips to 99.91% ($\rho = 40\%$), 98.74% ($\rho = 50\%$) and 91.64% ($\rho = 60\%$); the identical gentle downward trend persists for $n = 11$ through 13, underscoring the algorithm's stable degradation characteristic irrespective of dimension. Conversely, holding ρ constant and raising n consistently boosts TPR; for example, at $\rho = 60\%$ the value climbs from 91.64% ($n = 10$) to 96.43% ($n = 13$). This dimensional gain is attributed to the MM$*$ neighbor-pair validation mechanism, which exploits the larger number of candidate pairs available in higher dimensional hypercubes, thereby refining the propagation of fault-free labels and simultaneously suppressing

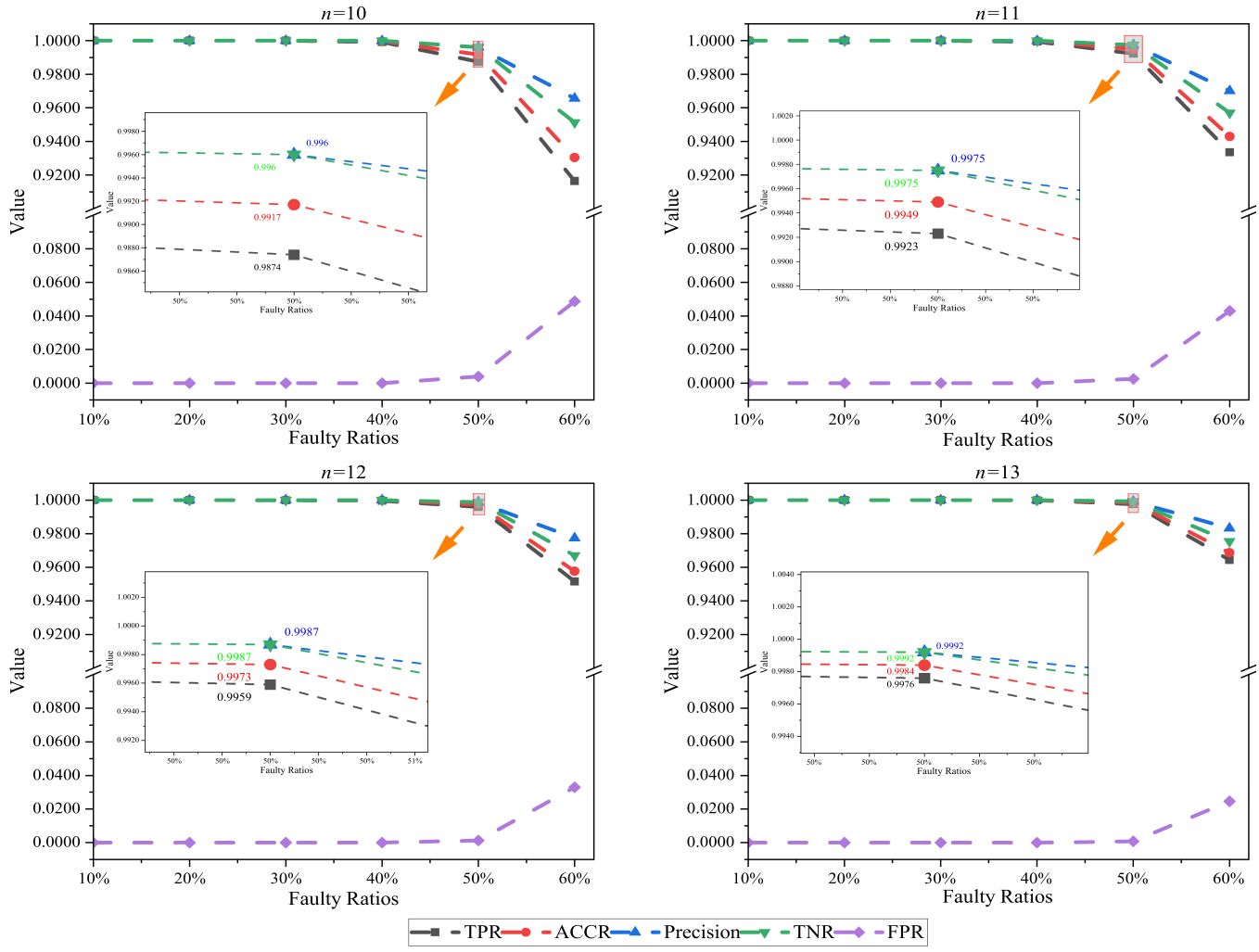

Fig. 9. Performance of FSFD-MM∗ on hypercube Q_n under varying faulty ratios.

TABLE IV
DIAGNOSTIC METRICS OF FSFD-MM∗ ON HYPERCUBE NETWORKS

Dimension	Faulty Ratios	Diagnostic Metrics				
n	ρ	TPR	ACCR	Precision	TNR	FPR
10	10%	1	1	1	1	0
	20%	1	1	1	1	0
	30%	1	1	1	1	0
	40%	0.9991	0.9996	0.9999	1	0
	50%	0.9874	0.9917	0.9960	0.9960	0.0040
	60%	0.9164	0.9304	0.9656	0.9513	0.0487
11	10%	1	1	1	1	0
	20%	1	1	1	1	0
	30%	1	1	1	1	0
	40%	0.9994	0.9997	0.9999	1	0
	50%	0.9923	0.9949	0.9975	0.9975	0.0025
	60%	0.9335	0.9429	0.9701	0.9570	0.0430
12	10%	1	1	1	1	0
	20%	1	1	1	1	0
	30%	0.9999	1	1	1	0
	40%	0.9996	0.9998	1	1	0
	50%	0.9959	0.9973	0.9987	0.9987	0.0013
	60%	0.9515	0.9577	0.9774	0.9670	0.0330
13	10%	1	1	1	1	0
	20%	1	1	1	1	0
	30%	1	1	1	1	0
	40%	0.9999	0.9999	1	1	0
	50%	0.9976	0.9984	0.9992	0.9992	0.0008
	60%	0.9643	0.9687	0.9833	0.9754	0.0246

FPR. Specifically, when ρ is fixed at 60% , FPR falls from 4.87% to 2.46% as n increases from 10 to 13, further confirming the algorithm's enhanced precision in larger networks.

In summary, both TSFD-PMC and FSFD-MM∗ demonstrate exceptional capabilities in fault diagnosis for hypercube networks. TSFD-PMC excels in handling high fault ratios (up to 60%), maintaining consistently high TPR ($> 99.5\%$) in all dimensions, ensuring robust detection even under extreme fault scenarios. FSFD-MM∗ shines in low to moderate fault scenarios ($\leq 40\%$), achieving near-perfect TPR (close 100%) and significantly lower FPR, with its performance improving more notably as network dimension increases. Together, they offer reliable, efficient diagnostic solutions tailored to diverse fault conditions, validating their effectiveness for large-scale HPC systems.

To quantify the advance achieved by the present work, we summarize the exact values of all major diagnosability metrics previously established for the hypercube Q_n under the two models in Table V. From Table V, the classical diagnosability grows only linearly with n, whereas our newly derived g-good-neighbor r-component diagnosability reaches $8n - 21$ when $g = 2, r = 2$, and $n \geq 24$—a value that is approximately eight

TABLE V
DIAGNOSABILITY METRICS FOR THE HYPERCUBE Q_n

Diagnosability Metric	**PMC Model**	**MM* Model**
classical diagnosability	n $(n \geq 3)$[27]	n $(n \geq 5)$[28]
conditional diagnosability	$4n-7$ $(n \geq 5)$[29]	$3n-5$ $(n \geq 5)$[30]
g-good-neighbor diagnosability	$(n-g+1)2^g-1$ $(n \geq 3, 0 \leq g \leq n-3)$[4]	$(n-g+1)2^g-1$ $(n \geq 5, 0 \leq g \leq n-3)$[31]
r-component diagnosability	$-\frac{1}{2}r^2+(n-\frac{1}{2})r+1$ $(n \geq 7, 0 \leq r \leq n)$[6]	$-\frac{1}{2}r^2+(n-\frac{1}{2})r+1$ $(n \geq 7, 0 \leq r \leq n)$[6]
h-extra diagnosability	$(h+1)n-h-\frac{h(h-1)}{2}$ $(n \geq 4, 0 \leq h \leq n)$[5]	$(h+1)n-h-\frac{h(h-1)}{2}$ $(n \geq 5, 1 \leq h \leq \frac{n-1}{4})$[32]
g-good-neighbor r-component diagnosability	$8n-21$ $(g=2, r=2, n \geq 24)$ **(This work)**	$8n-21$ $(g=2, r=2, n \geq 24)$ **(This work)**

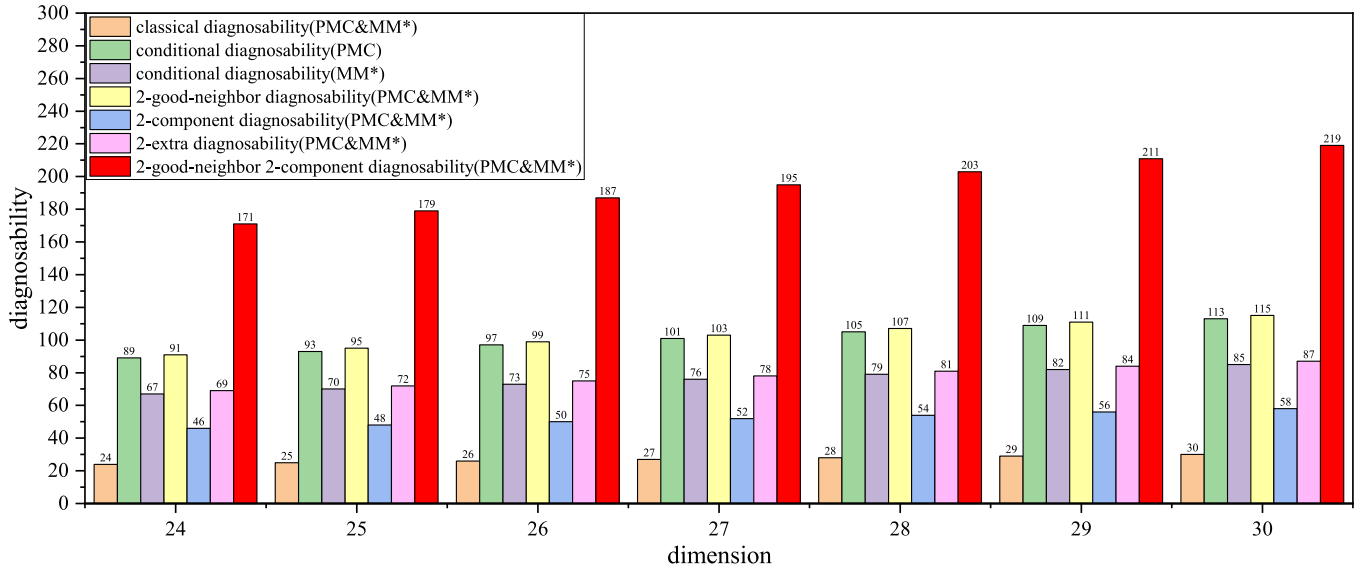

Fig. 10. Comparison of diagnosability metrics on the hypercube Q_n for $n = 24 \sim 30$ under the PMC and MM$*$ models.

times the classical diagnosability, four times the 2-component diagnosability, and twice the 2-good-neighbor diagnosability. This gain stems from simultaneously enforcing local connectivity of each node and global partitioning of the residual graph, two conditions that were previously studied only in isolation. Consequently, the g-good-neighbor r-component diagnosability significantly enhances network fault tolerance without additional hardware overhead. This advantage is visually confirmed in Fig. 10: the bars for 2-good-neighbor 2-component diagnosability steadily tower over all competing metrics throughout $24 \leq n \leq 30$, corroborating both the quantitative gain and the practical relevance of the proposed metric.

VI. CONCLUSION

In this work, we propose a novel diagnosis metric $D_{g,r}(G)$, which characterizes both the local node connectivity and the global partitioning of the network. Specifically, we apply the diagnosis measurement in the n-dimensional hypercube network Q_n under both the PMC and MM$*$ diagnostic models, and characterize the diagnosability of the 2-good-neighbor 2-component ($D_{2,2}$) for Q_n. Through rigorous analysis, we have proven that $D_{2,2}(Q_n) = 8n-21$ holds for $n \geq 24$. Using the structural properties inherent to these models, we develop two scalable multistage fault diagnosis algorithms, TSFD-PMC and FSFD-MM$*$, specifically designed for regular interconnection topologies. Comprehensive simulation studies conducted on hypercube networks demonstrate the high efficacy of both algorithms. When the fault node ratio is below 20% , both TSFD-PMC and FSFD-MM$*$ achieve approximately perfect identification (TPR $\approx 100\%$). Interestingly, in extreme fault scenarios that approach 50% , the algorithms maintain exceptional reliability, with TPR values exceeding 99.5% for TSFD-PMC and 98.7% for FSFD-MM$*$. These results robustly validate the operational efficacy of the proposed metrics and the associated framework for fault identification in large-scale HPC systems.

Future work will focus on two primary directions: 1) generalize the g-good-neighbor r-component diagnosability framework to data center networks, and 2) implement hardware-in-the-loop validation using the two algorithms to assess real-time fault diagnosis capabilities in operational scenarios. Theoretical extensions will focus on tightening diagnosability bounds through advanced graph polynomial techniques, while applied research will explore integration with emerging network-on-chip architectures.

Declaration of competing interest

The authors declare that there is no conflict of interest regarding the publication of this article.

REFERENCES

[1] F. P. Preparata, G. Metze, and R. T. Chien, "On the connection assignment problem of diagnosable systems," *IEEE Trans. Electron. Comput.*, vol. EC- 16, no. 6, pp. 848–854, Dec. 1967.

[2] J. Maeng and M. Malek, "A comparison connection assignment for self-diagnosis of multiprocessor systems," in *Proc. 11th Int. Symp. Fault-Tolerant Comput.*, Jun. 1981, Art. no. 175.

[3] A. Sengupta and A. T. Dahbura, "On self-diagnosable multiprocessor systems: Diagnosis by the comparison approach," *IEEE Trans. Comput.*, vol. 41, no. 11, pp. 1386–1396, Nov. 1992.

[4] S.-L. Peng, C.-K. Lin, J. J. M. Tan, and L.-H. Hsu, "The g-good-neighbor conditional diagnosability of hypercube under PMC model," *Appl. Math. Comput.*, vol. 218, no. 21, pp. 10406–10412, Jul. 2012.

[5] S. Zhang and W. Yang, "The g-extra conditional diagnosability and sequential t/k-diagnosability of hypercubes," *Int. J. Comput. Math.*, vol. 93, no. 3, pp. 482–497, Mar. 2016.

[6] S. Zhang, D. Liang, L. Chen, R. Li, and W. Yang, "The component diagnosability of hypercubes with large-scale faulty nodes," *Comput. J.*, vol. 65, no. 5, pp. 1129–1143, May. 2022.

[7] S. Zhang, D. Li, and H. Liu, "On g-extra conditional diagnosability of twisted hypercubes under MM$*$ model," *Int. J. Found. Comput. Sci.*, vol. 31, no. 4, pp. 445–459, Jun. 2020.

[8] H. Zhang, S. Zhou, J. Liu, Q. Zhou, and Z. Yu, "Reliability evaluation of dqcube based on g-good neighbor and g-component fault pattern," *Discrete Appl. Math.*, vol. 305, pp. 179–190, Dec. 2021.

[9] J. Liu, S. Zhou, D. Wang, and H. Zhang, "Component diagnosability in terms of component connectivity of hypercube-based compound networks," *J. Parallel Distrib. Comput.*, vol. 162, pp. 17–26, Apr. 2022.

[10] Y. Huang, K. Wen, L. Lin, L. Xu, and S.-Y. Hsieh, "Component fault diagnosability of hierarchical cubic networks," *ACM Trans. Des. Autom. Electron. Syst.*, vol. 28, no. 39, pp. 1–19, Mar. 2023.

[11] A. Sardroud and M. Ghasemi, "The g-good-neighbor diagnosability of triangle-free graphs," *J. Supercomput.*, vol. 79, no. 7, pp. 7272–7285, Mar. 2023.

[12] B. Zhu, S. Zhang, J. Zou, and C. Ye, "Two kinds of conditional connectivity of hypercubes," *AKCE Int. J. Graphs Combinatorics*, vol. 19, no. 3, pp. 255–260, Sep. 2022.

[13] F. Liao, J. Liu, C.-W. Lee, S.-Y. Hsieh, and J. Wu, "A novel adaptive system-level fault self-diagnosis algorithm and its applications," *IEEE Trans. Rel.*, vol. 74, no. 3, pp. 4294–4305, Sep. 2025.

[14] W. Liu, J. Liu, J.-M. Chang, J. Wu, and Q. Wang, "A novel fault-tolerant technique for star graph-based interconnection networks," *J. Supercomput.*, vol. 81, no. 7, May. 2025, Art. no. 820.

[15] J. Xu, Q. Zhu, X. Hou, and T. Zhou, "On restricted connectivity and extra connectivity of hypercubes and folded hypercubes," *J. Shanghai Jiaotong Univ.*, vol. 10, no. 2, pp. 203–207, Jun. 2005.

[16] Y. Saad and M. H. Schultz, "Topological properties of hypercubes," *IEEE Trans. Comput.*, vol. 37, no. 7, pp. 867–872, Jul. 1988.

[17] G. Ge, J. Liu, D. Wang, J. Wu, and G. Li, "A novel fault diagnostic algorithm with multiple characteristics for multiprocessor systems," *Theor. Comput. Sci.*, vol. 1045, Aug. 2025, Art. no. 115281.

[18] Q. Chen, J. Liu, C.-W. Lee, J. Wu, and G. Li, "The reliability of (n, k)-star network in terms of non-inclusive fault pattern," *Theor. Comput. Sci.*, vol. 1039, Jun. 2025, Art. no. 115189.

[19] Z. Wang, J. Liu, C.-W. Lee, J. Wu, and G. Li, "An analysis on component reliability of (n, k)-star networks," *J. Supercomput.*, vol. 81, no. 4, Mar. 2025, Art. no. 626.

[20] E. Cheng, Y. Mao, K. Qiu, and Z. Shen, "A general approach to deriving diagnosability results of interconnection networks," *Int. J. Parallel Emergent Distrib. Syst.*, vol. 37, no. 4, pp. 369–397, Jul. 2022.

[21] M.-J.-S. Wang, D. Xiang, and S.-Y. Hsieh, "G-good-neighbor diagnosability under the modified comparison model for multiprocessor systems," *Theor. Comput. Sci.*, vol. 1028, Feb. 2025, Art. no. 115027.

[22] N.-W. Chang and S.-Y. Hsieh, "Conditional diagnosability of enhanced hypercubes under the PMC model," *IEEE Trans. Netw.*, vol. 33, no. 4, pp. 1603–1613, Aug. 2025.

[23] H. Zhang, S. Zhou, E. Cheng, and S.-Y. Hsieh, "Characterization of cyclic diagnosability of regular diagnosable networks," *IEEE Trans. Rel.*, vol. 73, no. 1, pp. 270–278, Mar. 2024.

[24] N. Zhuo, S. Zhang, J.-M. Chang, and C. Ye, "Non-inclusive g-extra diagnosability of regular networks under the MM$*$ model," *J. Appl. Math. Comput.*, vol. 71, no. 4, pp. 5531–5553, Mar. 2025.

[25] X. Yang, D. J. Evans, and G. M. Megson, "On the maximal connected component of a hypercube with faulty vertices III," *Int. J. Comput. Math.*, vol. 83, no. 1, pp. 27–37, Jan. 2006.

[26] X. Liu, H. Liu, Y. Wang, B. Cheng, J. Fan, and G. Wang, "Fault tolerance of circulant-based recursive networks built on g-good neighbor fault pattern," *IEEE Trans. Rel.*, vol. 74, no. 4, pp. 5647–5659, Dec. 2025.

[27] J. R. Armstrong and F. G. Gray, "Fault diagnosis in a boolean n cube array of microprocessors," *IEEE Trans. Comput.*, vol. C- 30, no. 8, pp. 587–590, Aug. 1981.

[28] D. Wang, "Diagnosability of hypercubes and enhanced hypercubes under the comparison diagnosis model," *IEEE Trans. Comput.*, vol. 48, no. 12, pp. 1369–1374, Dec. 1999.

[29] P.-L. Lai, "Conditional diagnosability measures for large multiprocessor systems," *IEEE Trans. Comput.*, vol. 54, no. 2, pp. 165–175, Feb. 2005.

[30] G.-H. Hsu, C.-F. Chiang, L.-M. Shih, L.-H. Hsu, and J. J. M. Tan, "Conditional diagnosability of hypercubes under the comparison diagnosis model," *J. Syst. Architecture*, vol. 55, no. 2, pp. 140–146, Feb. 2009.

[31] S. Wang and W. Han, "The g-good-neighbor conditional diagnosability of n-dimensional hypercubes under the MM$*$ model," *Inf. Process. Lett.*, vol. 116, no. 9, pp. 574–577, Sep. 2016.

[32] A. Liu, S. Wang, J. Yuan, and J. Li, "On g-extra conditional diagnosability of hypercubes and folded hypercubes," *Theor. Comput. Sci.*, vol. 704, pp. 62–73, Dec. 2017.

Yuankang Mao received the B.E. degree in software engineering from Wuhan University of Technology, Wuhan, China, in 2021. He is currently working toward the master's degree in computer science and technology with Guangxi Normal University, Guilin, China.

His research interests include network reliability, fault tolerant computing, and algorithms.

Jiafei Liu received the B.S. degree in applied mathematics from Zhoukou Normal University, Zhoukou, China, in 2017, and the Ph.D. degree in cyberspace security from Fujian Normal University, Fuzhou, China, in 2022.

He is currently working with the School of Computer Science and Engineering, Guangxi Normal University. He was awarded for the Guangxi Qingmiao Talent Program in 2024 and the Guangxi Young Elite Scientists Sponsorship Program in 2025. He has published more than 30 papers and has served as a positive reviewer including IEEE TRANSACTIONS ON COMPUTERS, IEEE TRANSACTIONS ON RELIABILITY, Theoretical Computer Science, Computer Journal and other publications. His research interests include network reliability, fault tolerant computing, algorithms, and interconnection networks.

Sun-Yuan Hsieh (Fellow, IEEE) received the Ph.D. degree in computer science from National Taiwan University, Taipei, Taiwan, in June 1998.

He is now a Chair Professor with the Department of Computer Science and Information Engineering, National Cheng Kung University, Tainan. His research interests include design and analysis of algorithms, fault-tolerant computing, bioinformatics, parallel and distributed computing, and algorithmic graph theory.

Dr. Hsieh was a recipient of the number of awards including the 2020 ACM Distinguished Scientist, 2019 Kwoh Ting Li Honorable Scholar Award, 2016 Outstanding Research Award of Taiwan Ministry of Science and Technology, President's Citation Award (American Biographical Institute), in 2007, and Outstanding Engineering Professor Award of Chinese Institute of Engineers, in 2014. He is a fellow of the British Computer Society and a fellow of the Institution of Engineering and Technology. He is currently an experienced Editor with editorial services to a number of journals, including serving as an Associate Editor for IEEE TRANSACTIONS ON COMPUTERS, IEEE TRANSACTIONS ON RELIABILITY, IEEE ACCESS, *Journal of Computer and System Science*, Theoretical Computer Science, Discrete Applied Mathematics, Journal of Supercomputing, Editor-in-Chiefs of the International Journal of Computer Mathematics, Parallel Processing Letters, Discrete Mathematics, Algorithms and Applications, and the Managing Editor for the Journal of Interconnection Networks.

Jingli Wu received the B.S. degree in computer software, the M.S. degree in control theory and control engineering from Guangxi University, Guangxi, China, and the Ph.D. degree in computer application from Central South University, Changsha, China, in 2000, 2003, and 2008, respectively.

She is a Professor with the College of Computer Science and Information Engineering, Guangxi Normal University. Her current research focuses on bioinformatics, intelligent optimization algorithm.

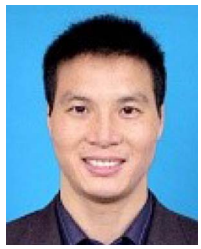

Gaoshi Li received the Ph.D. degree in computer science and technology from Central South University, Changsha, China, in 2019.

He is currently an Associate Professor with Key Lab of Education Blockchain and Intelligent Technology, Ministry of Education & Guangxi Key Lab of Multi-source Information Mining & Security and College of Computer Science and Engineering, Guangxi Normal University. His current research interests include bioinformatics, computational biology, and machine learning.